

Enhanced localization, energy anomalous diffusion and resonant mode in harmonic chains with correlated mass-spring disorder

S S de Albuquerque¹, J L L dos Santos², F A B F de Moura²
and M L Lyra²

¹ Curso de Física, Universidade Federal de Alagoas, Campus Arapiraca, Arapiraca—AL, 57309-005, Brazil

² Instituto de Física, Universidade Federal de Alagoas, Maceió AL 57072-970, Brazil

E-mail: fidelis@fis.ufal.br

Received 12 January 2015, revised 3 March 2015

Accepted for publication 10 March 2015

Published 2 April 2015



CrossMark

Abstract

In this work, we study the vibrational modes and energy spreading in a harmonic chain model with diluted second-neighbors couplings and correlated mass-spring disorder. While all nearest neighbor masses are coupled by an elastic spring, second neighbors springs are introduced with a probability p_D . The masses are randomly distributed according to the site connectivity $m_i = m_0 (1 + 1/n_i^\alpha)$, where n_i is the connectivity of the site i and α is a tunable exponent. We show that maximum localization of the vibrational modes is achieved for $\alpha \simeq 3/4$. The time-evolution of the energy wave-packet is followed after an initial localized excitation. While the participation number remains finite, the energy spread is shown to be sub-diffusive after a displacement and super-diffusive after an impulse excitation. These features are related to the development of a power-law tail in the wave-packet distribution. Further, we unveil that the spring dilution leads to the emergence of a resonant localized state which is signaled by a van Hove singularity in the density of states.

Keywords: disorder, vibrational modes, localization

(Some figures may appear in colour only in the online journal)

1. Introduction

The Anderson localization phenomenon is ubiquitous to any wave-like excitation that propagates in random media [1–5]. In particular, the nature of eigenmodes in non-periodic classical lattices is a very interesting issue with several lines of investigation [6–25, 29]. It is well known that the energy flux in low-dimensional non-periodic classical lattices is strongly dependent on the localized/extended nature of the vibrational modes. Dyson [30] showed that the vibrational eigenstates of a one-dimensional disordered harmonic chain with N random masses can be mapped onto the one-electron tight-binding model [6]. Most of the normal vibrational modes are localized, except a few low-frequency modes whose number is of the order of \sqrt{N} [6, 19]. Furthermore, by using analytical arguments, the transport of energy in

mass-disordered harmonic chains is directly related to the delocalized vibrational modes, also termed non-scattered modes as they are not influenced by the underlying disorder, as well as on the initial excitation [20]. Calculations indicated that uncorrelated random chains have a super-diffusive behavior for the second moment of the energy distribution [$M_2(t) \propto t^{1.5}$] for impulse initial excitations, while for initial displacement excitations a sub-diffusive spread takes place [$M_2(t) \propto t^{0.5}$]. The dependence of the second moment spread on the initial excitation was also obtained in [31].

It has been demonstrated that the above framework can change when some correlations are introduced in the disorder distribution [21–25]. A new set of high-frequency delocalized modes emerge when short [21, 22] or long-range correlations [23–25] are introduced in the disorder distribution

(spring constants or masses). A phase of low-energy extended collective excitations was observed in the regime of strong long-range correlations in the mass distribution [23]. Recently, the effect of short-range correlations in the mass distribution on the heat conduction through harmonic chains was investigated [26]. It has been unveiled that high and low-frequency modes are affected quite differently. While the high-frequency modes become more extended, there is an overall tendency of enhanced localization of the low-frequency modes. Therefore, the effect of correlations on the localization of harmonic excitations is quite non-trivial and new insights are in order to properly develop a deeper understanding of its underlying physical mechanisms.

In this work, we contribute along this research line by introducing a disordered harmonic chain model with correlated random masses and connectivities. The model consists of a linear harmonic chain with first and second neighbors couplings. All first neighbors springs are present but only a fraction p_D of the second neighbor ones. Therefore, each mass can be connected with two, three or four other masses. In order to couple the disorder in the connectivity to the mass distribution, we consider the i -th mass to be given by $m_i = m_0 (1 + 1/n_i^\alpha)$, where m_0 is a reference mass, n_i is the connectivity of the site i and α is a tunable parameter.

Such power-law relation between the local connectivity and mass allows for a straightforward extension for the case of harmonic chain models with long-range couplings without the need of introducing any characteristic connectivity scale. These models have been shown to be associated with the problem of optimal synchronization of vibrational waves [27] and mode localization in the presence of cost limitations [28].

By using exact diagonalization on finite lattices, we calculate the participation number within the allowed frequencies band. We will show that the correlation between the mass and connectivity disorders, controlled by the parameter α , can be tuned to achieve a maximum enhancement of Anderson localization, without affecting the sub and super-diffusive character of initially localized excitations. The dynamical scaling behavior of the wave-packet will also be characterized. Further, we will show that there is a set of localized modes at a resonance frequency that is signaled as a van Hove singularity in the density of states.

2. Model and formalism

We will consider a one-dimensional chain with N masses connected by harmonic springs. In this chain model, all nearest neighbors are connected by a spring with elastic constant k_0 . Additional springs, coupling directly second neighbors, are also introduced. However, only a fraction p_D of the second neighbor masses are randomly chosen to be coupled by a direct spring. In order to correlate the mass distribution with the disordered connectivity distribution, the masses are chosen according to

$$m_i = m_0 (1 + 1/n_i^\alpha) \quad (1)$$

where n_i represents the number of springs connected to site i , m_0 is a reference mass and α is a tunable parameter that controls

the degree of correlation between the connectivity and mass random distribution. In the limits of $\alpha = 0$ and $\alpha \rightarrow \infty$ disorder remains restricted to the connectivity distribution. The equation of motion for the i -th mass is given by:

$$m_i \frac{d^2 q_i}{dt^2} = \sum_{i \neq j} k_{i,j} (q_i - q_j) \quad (2)$$

In this model, we have:

$$k_{i,j} = \begin{cases} k_0 & \text{if } |i - j| = 1 \\ \frac{1}{2} k_0 \theta(p - p_D) & \text{if } |i - j| = 2 \\ 0 & \text{otherwise} \end{cases}$$

where $\theta(x)$ is the Heaviside function and p is a random number uniformly distributed within the interval $[0, 1]$. The second neighbors dilution probability is kept equal to $p_D = 1/2$. The second neighbors elastic constant is taken to be $k_0/2$ to account for the size dependence of the spring deformation. The phenomenology we are going to explore remains qualitatively the same for other dilution fractions. We will apply two distinct formalisms to study the vibrational modes and the energy flux of this model. To study the energy dynamics we consider that the fraction of the total energy H_0 at site (i) is given by $f_i(t) = h_i(t)/H_0$ where $h_i(t)$ is the energy of the mass at site (i). In the case of a uniform energy packet spread over a chain with N sites, we have $f_i \approx 1/N$. Therefore, we can define the generalized time-dependent participation number

$$\xi(t) = \frac{1}{\sum_i f_i^2} \quad (3)$$

$\xi = N$ for a uniform energy packet. Thus, the function ξ is a measure of the number of masses that effectively participate of the energy transport. In our calculations, an initial excitation is introduced at the center of the chain, i.e. the site $(N/2)$. We will also compute the second moment of the energy distribution, $M_2(t)$, defined by [20]

$$M_2(t) = \sum_{i=1}^N (i - i_0)^2 [f_i(t)], \quad (4)$$

The second moment of the energy distribution $M_2(t)$ has the same status of the mean-square displacement of the wave-packet of an electron in a solid [20, 31]. We solved equation (2) by using the standard Runge-Kutta algorithm to obtain $\xi(t)$ and $M_2(t)$.

The vibrational normal modes can be obtained through the exact diagonalization of the secular matrix Ω , where $\Omega_{i,i} = (k_{i,i+1} + k_{i,i-1} + k_{i,i+2} + k_{i,i-2})/m_i$, $\Omega_{i,i+1} = \Omega_{i+1,i} = -k_{i+1,i}/\sqrt{(m_{i+1}m_i)}$, $\Omega_{i,i+2} = \Omega_{i+2,i} = -k_{i+2,i}/\sqrt{(m_{i+2}m_i)}$ and all other $\Omega_{i,j} = 0$. The spatial extension of those eigenstates can be obtained by calculating their participation number defined by [32]:

$$\xi(\omega^2) = \frac{\sum_{i=1}^N u_i^2(\omega^2)}{\sum_{i=1}^N u_i^4(\omega^2)}, \quad (5)$$

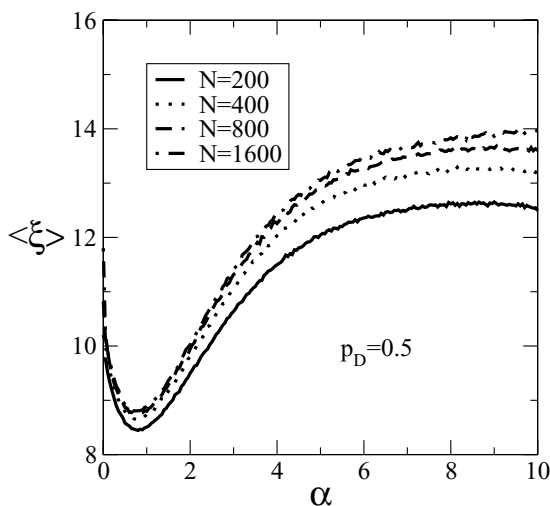


Figure 1. Average participation number versus α for $N = 200, 400, 800$ and 1600 . Calculations were done for 1000 samples and $m_0 = 2$. Notice that a stronger localization appears for $\alpha \simeq 0.75$.

where the u_i 's are the coefficients of the eigenstate of frequency ω . The participation number scales proportional to the system size for extended states and is finite for exponentially localized modes.

3. Results and discussions

We applied an exact diagonalization procedure on finite chains with $N = 200$ up to 1600 sites. All calculations were averaged over, at least, 1000 disorder configurations. In figure 1 we plot the average participation number $\langle \xi \rangle$ versus the exponent α . Calculations were done for $m_0 = 2$ (in units of an arbitrary elementary mass m_u). The averaged participation number $\langle \xi \rangle$ was obtained by using an arithmetic average of all participation within the entire band except the frequencies at the vicinity of $\omega = 0$. We observe that the participation number exhibits a non-monotonic behavior with a minimum around $\alpha \approx 0.75$. In this case, the correlation between the connectivity and mass distributions leads to the strongest enhancement of Anderson localization, with the average participation number being roughly 1/2 of the one obtained in the absence of mass-dilution correlation. In the following, we are going to explore the characteristics of the eigestates and energy spreading in such extremal case.

In figure 2 we analyze the spectrum of the participation number as a function of the mode frequency. We plot ξ versus ω^2 (in units of k_0/m_u) for $N = 200$ up to 1600 sites, and the particular extremal case of $\alpha = 3/4$. Notice that only the uniform mode ($\omega = 0$) has the participation number proportional to N , i.e. the introduction of second nearest neighbor couplings does not promote the appearance of new extended modes. It is important to notice that a strongly localized mode appears at a specific high-frequency, evidenced in the figure inset. The nature of these strongly localized modes will be discussed in the end of this section.

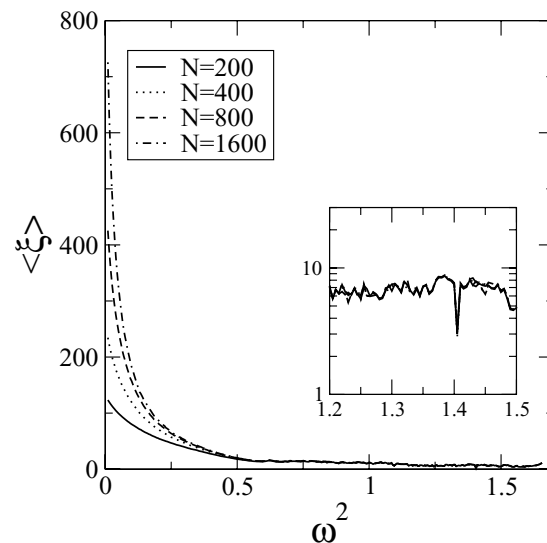


Figure 2. Spectrum of the participation number as a function of the squared mode frequency ω^2 for $N = 200$ up to 1600 sites, at the particular case of $\alpha = 3/4$. All modes, except the uniform $\omega = 0$ one are localized, irrespective of the presence of mass-spring correlations. There appears a strongly localized mode at a resonance frequency $\omega^2 \simeq 1.4$, as evidenced in the inset.

To follow the time-evolution of an initially localized excitation, we solved equation (2) for an initially localized energy pulse. We considered two distinct types of initial excitation: a displacement excitation defined by $q_i(t=0) = \delta_{i,N/2}$ and $\dot{q}_i = 0$; and an impulse excitation defined by $\dot{q}_i = \delta_{i,N/2}$ and $q_i = 0$. It was shown in the previous literature that these two initial conditions lead to quite distinct energy spreading dynamics [23, 24]. The spectral decomposition of an impulse excitation has a large contribution coming from the weakly localized low-frequency modes, which results in a super-diffusive spreading. On the other hand, a displacement excitation has weaker low-frequency modes and its spreading is slower (sub-diffusive). We used a fourth order Runge-Kutta method with $\delta t = 0.001$ and a chain with $N = 20\,000$ masses. The energy conservation was checked to ensure numerical precision. In figures 3(a) and (b) we plot the time-dependent mean-square displacement M_2 and the participation number $\xi(t)$ versus t for $\alpha = 3/4$ and a displacement initial excitation. Our results for $M_2(t)$ indicate a sub-diffusive spreading dynamics at long times $M_2(t) \propto t^{0.5}$. This result agrees with previous results found in harmonic chains with disordered masses and nearest neighbors interactions. The uniform mode $\omega = 0$ promotes the slow divergence of the energy wave-packet width. However, the time-dependent participation number saturates in a finite value thus being dominated by localized eigenmodes. This feature supports previous findings showing that a finite fraction of the energy packet remains trapped near the initial site in a disordered harmonic chain with nearest neighbors couplings [20]. Our calculations indicate that the presence of second-neighbors couplings and mass-spring correlations do not change this framework. We also addressed the case of an impulse initial excitation ($\dot{q}_i(t=0) = \delta_{i,N/2}$ and $q_i = 0$). In this case $M_2(t)$

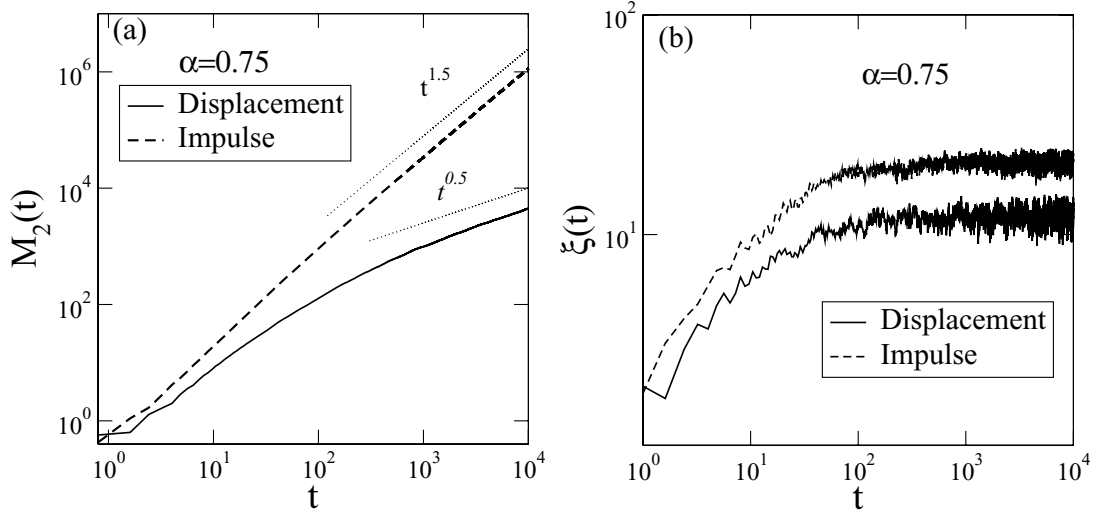


Figure 3. (a) Time dependent mean square displacement M_2 and (b) the participation number $\xi(t)$ versus time t for $\alpha = 3/4$. Calculations were done for $N = 20\,000$ sites for both initial displacement and impulse excitations.

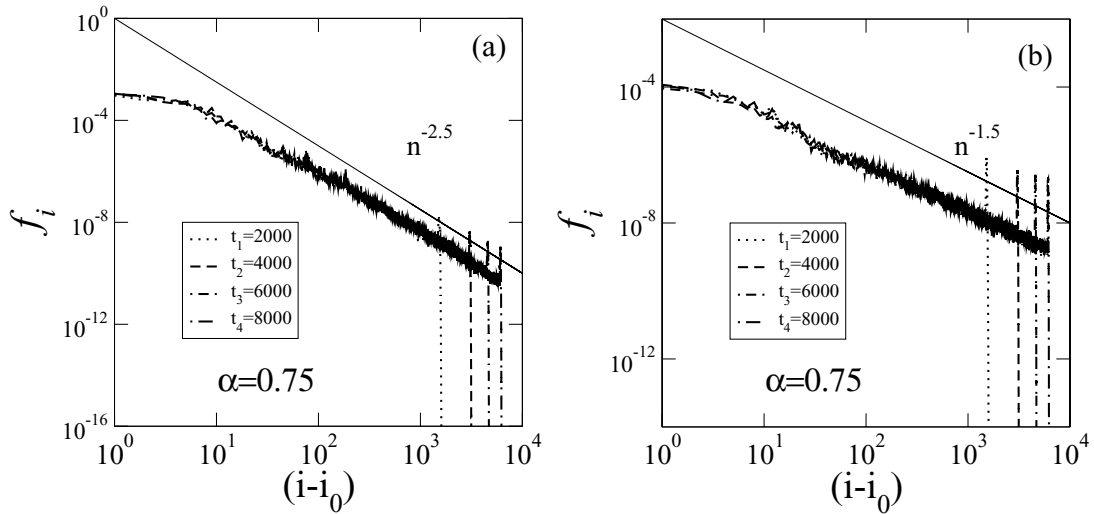


Figure 4. Energy profile $f_i \times (i - i_0)$ with $i > i_0$ at four distinct times $t = 2000, 4000, 6000$ and 8000 . Calculations were done for the correlation exponent $\alpha = 3/4$ by using (a) $N = 20\,000$ sites and an initial displacement excitation $q_i = \delta_{i,N/2}$ and (b) $N = 30\,000$ sites and an initial impulse excitation $\hat{q}_i = \delta_{i,N/2}$.

displays a super-diffusive spread $M_2(t) \propto t^{1.5}$ at long times. Although reaching a larger value, the participation number still saturates.

In order to develop a deeper understanding of the above dynamical behavior, we report the energy profile $f_i \times (i - i_0)$ with $i > i_0$ at four distinct times $t = 2000, 4000, 6000$ and 8000 (see figures 4(a) and (b)). Calculations were done for figure 4(a) an initial displacement excitation and figure 4(b) an initial impulse excitation. We observe that the energy profile develops a power-law tail $f_i \propto (i - i_0)^{-\phi}$ for $0 < (i - i_0) < n^*$. Here, n^* represents the energy wave-packet front. Due to the finite propagation velocity of the low-frequency modes, this cutoff grows linearly in time ($n^* \propto t^\beta$ with $\beta = 1$). The power-law exponent governing the decay of the energy wave-packet is found to be $\phi = 2.5$ in figure 4(a) and $\phi = 1.5$ in figure 4(b).

The scaling behavior of the mean-square displacement and participation number can be computed analytically by following heuristic arguments. We consider the wave-packet to scale as $f_i(t) = f_0(t) f((i - i_0)/n^*)$ with $f((i - i_0)/n^*) \propto (i - i_0)^{-\phi}$. In our calculations, a finite fraction of the initial energy remains trapped close to the initial site, which means that $f_0(t) \propto \text{constant}$. It is then straightforward to show that the mean squared displacement shall scale as $M_2(t) \propto t^{\beta(3-\phi)}$. The exponents governing the power-law tail of the energy distribution ($\phi = 2.5$ for the case of an initial displacement excitation and $\phi = 1.5$ for an initial impulse excitation) are in full agreement with the respectively reported sub-diffusive and super-diffusive spread of the wave-packet second moment. The saturation of participation number can also be understood following the same scaling argument. It can be written as

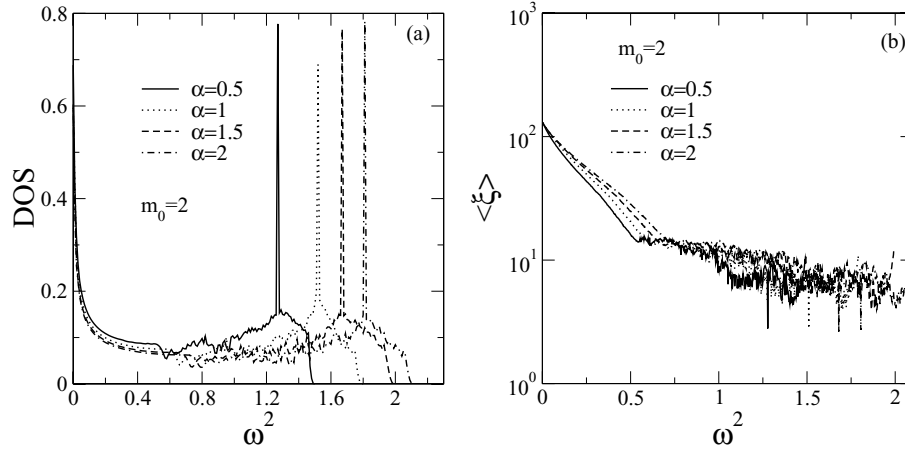


Figure 5. (a) The vibrational density of states (DOS) versus ω^2 for chains with $N = 4000$ sites, 1000 distinct disorder configuration, $\alpha = 0.25$ up to 1. We observe that the DOS exhibits a narrow peak in the high frequency region signaling a van Hove singularity associated with an underlying symmetry. (b) The corresponding spectra of the participation number showing that the resonance mode is strongly localized.

$\xi \approx \xi_0 + [\int_0^{\omega^*} (f_i)^2 di]^{-1}$. ξ_0 is a constant that represent the participation of the energy fraction trapped close to the initial site. ξ_0 is of the order of few lattice spacings. The contribution coming from the integral over the wave-packet tail is finite in the cases of displacement and impulse excitations, both having $\phi > 1/2$. Therefore, $\xi(t \rightarrow \infty)$ shall remain finite, in agreement with the previous results from the direct numerical integration of the motion equations.

Before finishing, we would like to discuss the nature of the strongly localized mode appearing in the spectrum of the participation number reported in figure 2. We start by computing the density of states (DOS) through an exact diagonalization to obtain the complete frequency spectrum. The DOS is numerically computed as $\text{DOS}(\omega^2) = \sum_{\omega_i} \delta(\omega_i^2 - \omega^2)$. In figure 5 we plot the DOS versus ω^2 for $N = 4000$ sites, 1000 distinct disorder configuration, $\alpha = 0.5, 1, 1.5, 2$ and $m_0 = 2$. For $\omega \approx 0$ the density of states displays the typical divergence associated with the uniform mode. However, the DOS depicts also a diverging singularity at a high frequency. The DOS singularity is at the same frequency on which the participation number has a pronounced deep (as shown in figure 5(b)) for all values of α . These features indicate that this frequency corresponds to degenerated strongly localized resonant modes. After considering some possible local configurations that may result in resonant localized modes, we found that this resonant mode is distributed in four nearest neighbor sites, with the following configuration of couplings: Due to the dilution of the second neighbor couplings, there is a finite probability of four consecutive sites to have no second-neighbor couplings among them, but the inner sites being coupled to sites outside this segment by second neighbor springs. No second neighbor springs are attached to the outer sites. In this case, there is a frequency on which the site displacements remain restricted to this segment. Introducing the harmonic mode $q_n = u_n \exp(i\omega t)$ in equation (2), this

localized mode obeys the following set of equations:

$$\begin{aligned} -m_n \omega^2 u_n &= \frac{5}{2} k_0 u_n - k_0 u_{n-1} - k_0 u_{n+1} \\ -m_{n-1} \omega^2 u_{n-1} &= 2k_0 u_{n-1} - k_0 u_n \\ -m_{n+1} \omega^2 u_{n+1} &= \frac{5}{2} k_0 u_{n+1} - k_0 u_{n+2} - k_0 u_n \\ -m_{n+2} \omega^2 u_{n+2} &= 2k_0 u_{n+2} - k_0 u_{n+1} \end{aligned} \quad (6)$$

The localized resonant mode has $u_{n-1} = -\frac{u_n}{2} = \frac{u_{n+1}}{2} = -u_{n+2}$. This excitation does not propagate outside this segment, once the resulting force on the outside neighboring sites remains null. This mode appears at the resonance frequency

$$\omega_0^2 = \frac{4k_0}{m_0(1+3^{-\alpha})}. \quad (7)$$

For example, for $m_0 = 2$ and $\alpha = 0.5$ this resonance frequency is, respectively $\omega_0^2 \approx 1.2679$, in agreement with the DOS and participation number singularities.

4. Summary and conclusions

In summary, we investigated the role of correlated disorder in harmonic chains with diluted second neighbors couplings. We introduced correlations between the disorder distribution in the second neighbors spring constants and the mass disorder by considering each mass as a function of the site connectivity given by $m_i = m_0 (1 + 1/n_i^\alpha)$, where n_i , is the connectivity of the site i and α is a tunable exponent. By using an exact diagonalization procedure on finite chains, we showed that the average participation number of the collective normal modes achieves a minimum at $\alpha \simeq 3/4$. This feature indicates that localization of vibrational modes can be enhanced by a proper manipulation of local correlations in the disorder distribution. This seems to be a quite general feature associated with the nature of collective excitations in lattices with correlated disorder and can be extended to tight-binding models with correlated diagonal and off-diagonal disorder. Further, we showed that, although the participation number of an initial localized excitation remains finite after a long time evolution,

the second moment of the energy distribution grows sub-diffusively for a displacement excitation and super-diffusively for an impulse excitation, even in the presence of second-neighbors couplings and local correlations. To develop a deeper understanding of the distinct dynamics exhibited by the wave-packet participation number and width, we followed the time-evolution of the energy distribution unveiling that it develops a power-law tail with distinct exponents for displacement and impulse initial excitations. We performed a detailed scaling analysis to relate the wave-packet scaling with the asymptotic behavior of the participation number and the wave-packet dispersion. Finally, we showed that there is a resonant frequency at which the normal modes are localized on a finite segment composed of four sites with a specific configuration of the local couplings that results in a null net force on the remaining chain. The presence of such resonant mode is reflected in the spectrum of the participation number as a pronounced deep, as well as a van Hove singularity on the density of states. We have analytically demonstrated the dependence of such resonant frequency on the exponent α correlating mass and spring disorder. It would be interesting to extend the present work to investigate the interplay between mass and spring disorder in higher-dimensional models that may have a band of extended modes. In this case, the correlation exponent could also be used to tune the width of the extended band.

Acknowledgments

This work was partially supported by CNPq, CAPES, and FINEP (Federal Brazilian Agencies), CNPq-Rede Nanobioestruturas, as well as FAPEAL (Alagoas State Agency).

References

- [1] Izrailev F M, Krokhnin A A and Makarov N M 2012 *Phys. Rep.* **512** 125
- [2] Kramer B and MacKinnon A 1993 *Rep. Prog. Phys.* **56** 1469
- [3] Abrahams E, Anderson P W, Licciardello D C and Ramakrishnan T V 1979 *Phys. Rev. Lett.* **42** 673
- [4] Romer R A and Schulz-Baldes H 2004 *Europhys. Lett.* **68** 247
- [5] Abrahams E 1998 *Physica E* **3** 69
- [6] Dean P 1964 *Proc. Phys. Soc.* **84** 727
- [7] Cressoni J C and Lyra M L 1996 *J. Phys.: Condens. Matter* **8** L83
- [8] Yan Y and Zhao H 2012 *J. Phys.: Condens. Matter* **24** 275401
- [9] Kundu A, Chaudhuri A, Roy D, Dhar A, Lebowitz J L and Spohn H 2010 *Europhys. Lett.* **90** 40001
- [10] Nika D L and Balandin A A 2012 *J. Phys.: Condens. Matter* **24** 233203
- [11] Li B, Zhao H and Hu B 2001 *Phys. Rev. Lett.* **86** 63
- [12] Dhar A 2001 *Phys. Rev. Lett.* **86** 5882
- [13] Garrido P L, Hurtado P I and Nadrowski B 2001 *Phys. Rev. Lett.* **86** 5486
- [14] Savin A V, Tsironis G P, and Zolotaryuk A V 2002 *Phys. Rev. Lett.* **88** 154301
- [15] Dhar A 2002 *Phys. Rev. Lett.* **88** 249401
- [16] Garrido P L and Hurtado P I 2002 *Phys. Rev. Lett.* **88** 249402
- [17] Roy D and Dhar A A 2008 *Phys. Rev. E* **78** 051112
- [18] Dhar A 2008 *Adv. Phys.* **57** 457
- [19] Shima H, Nishino S and Nakayama T 2007 *J. Phys.: Conf. Ser.* **92** 012156
- [20] Xiao J J, Yakubo K and Yu K W 2006 *Phys. Rev. B* **73** 054201
- [21] Xiao J J, Yakubo K and Yu K W 2006 *Phys. Rev. B* **73** 224201
- [22] Matsuda H and Ishii K 1970 *Prog. Theor. Phys. Suppl.* **45** 56
- [23] Ishii K 1973 *Prog. Theor. Phys. Suppl.* **53** 77
- [24] Datta P K and Kundu K 1995 *Phys. Rev. B* **51** 6287
- [25] Datta P K and Kundu K 1994 *J. Phys.: Condens. Matter* **6** 4465
- [26] Dominguez-Adame F, Maci E and Sánchez A 1993 *Phys. Rev. B* **48** 6054
- [27] de Moura F A B F, Coutinho-Filho M D, Raposo E P and Lyra M L 2003 *Phys. Rev. B* **68** 012202
- [28] Albuquerque S S, de Moura F A B F and Lyra M L 2005 *Physica A* **357** 165
- [29] de Moura F A B F and Domínguez-Adame F 2008 *Eur. Phys. J. B* **66** 165
- [30] Ong Z-Y and Zhang G 2014 *Phys. Rev. B* **90** 155459
- [31] Motter A E, Zhou C and Kurths J 2005 *Phys. Rev. E* **71** 016116
- [32] Morais P A, Andrade J S, Nascimento E M and Lyra M L 2011 *Phys. Rev. E* **84** 041110
- [33] de Moura F A B F 2010 *J. Phys.: Condens. Matter* **22** 435401
- [34] Dyson F 1953 *Phys. Rev.* **92** 1331
- [35] Wagner M, Zart G, Vazquez-Marquez J, Viliani G, Frizzera W, Pilla O and Montagna M 1992 *Phil. Mag. B* **65** 273
- [36] de Moura F A B F, Lyra M L, Malyshev V A, Domínguez-Adame F and Malyshev A V 2005 *Phys. Rev. B* **71** 174203